Quantification of Endothelin Receptor Subtypes in Peripheral Tissues Reveals Downregulation of ET_A Receptors in ET_B-Deficient Mice

RHODA E. KUC,[1] JANET J. MAGUIRE, AND ANTHONY P. DAVENPORT

Clinical Pharmacology Unit, University of Cambridge, Level 6, Addenbrooke's Centre for Clinical Investigation, Addenbrooke's Hospital, Cambridge CB2 2QQ, United Kingdom

We have previously shown that in homozygous endothelin $(ET)_B^{-/-}$deficient mice, ET_A receptor density is significantly downregulated in the brain by 45%. In these mice, plasma ET-1 levels are elevated. Our aim was to use quantitative autoradiography to establish the distribution of ET receptor subtypes in peripheral tissues from wild-type mice and to measure the density of the ET_A subtype in $ET_B^{-/-}$ knockout animals. Our second aim was to test whether deletion of ET_B receptors, which is associated with elevated plasma levels of ET-1, would also reduce ET_A expression in the periphery. In longitudinal sections from wild-type mice, the highest densities of ET_A receptors localized to major organs including the ventricle of the heart, lung, and liver parenchyma. High densities of ET_A receptors were detected in the smooth muscle layer of the vasculature such as intrarenal vessels as well as the smooth muscle layer and epithelial cells of the gastrointestinal tract. In these tissues, the ET_A subtype was more abundant, representing between 60% and 100% of the ET receptors. ET_B receptors predominated in the medulla of kidney, with high densities also localizing to glomeruli within the cortex and to the sinusoids from the liver. Lower densities of ET_B receptors were also present in the lung, heart, liver, and the smooth muscle layer of the gastrointestinal tract. In $ET_B^{-/-}$ knockout mice, ET_B receptors were not detected as expected by either ligand binding or immunocytochemistry. The pattern of ET_A receptor distribution in the $ET_B^{-/-}$ knockout mice was similar to the controls, but the density of ET_A receptors was significantly reduced in the lung by 39%. Diminished responses to the endogenous agonist after repeated stimulation are an important feature of G-protein signaling, preventing potential damage to the overstimulated cell, and it is likely that downregulation occurs in response to higher circulating levels of ET-1. Exp Biol Med 231:741–745, 2006

Key words: image analysis; knockout mouse; quantitative autoradiography; radioligand binding

The structure of endothelin-1 (ET-1) is unique among the mammalian bioactive peptides in containing two disulfide bridges, especially the bridge between Cys^1 and Cys^{15} residues, which may render the N-terminus less susceptible to aminopeptidases. This can confer increased resistance to degradation of the peptide by enzymatic pathways. ET-1 remains one of the most potent constrictors of human vessels with an unusually long-lasting action (1). Effective removal from the circulation of ET-1 by non-enzymatic pathways such as receptor internalization may be crucial, particularly under pathophysiological conditions, when circulating plasma levels may be elevated.

An important emerging role of the ET_B subtype is to function as a clearing receptor, removing ET-1 from the circulation (2, 3). We have recently shown using positron emission tomography to dynamically image ET receptors *in vivo*, that ET_B receptors in lungs, kidney, and, to a lesser extent, liver, efficiently clear ^{18}F-labeled ET-1 from the circulation to prevent the peptide binding to the heart (4). We speculated that ET_B receptors clear ET-1 from the circulation, thus protecting the heart from potentially deleterious actions of ET-1, mediated *via* the ET_A subtype. We have also shown that in human blood vessels removed from patients with pathophysiological conditions known to elevate plasma levels of ET-1, smooth muscle ET_A receptors are downregulated. We speculated that this may be the result of an adaptive response to high levels of agonist (5), because, unlike many transmitters, the ET system is characterized by a lack of ET_A receptor reserve (6). In agreement, in a rat model of acute hypertension in which adenovirus transfer of the pre-proET-1 gene significantly increased plasma ET-1 levels after 4 days, there was a

This study was supported by the British Heart Foundation.

[1] To whom correspondence should be addressed at Clinical Pharmacology Unit, University of Cambridge, Level 6, Addenbrooke's Centre for Clinical Investigation, Box 110, Addenbrooke's Hospital, Cambridge CB2 2QQ, UK. E-mail: rek22@medschl.cam.ac.uk

Received September 29, 2005.
Accepted November 7, 2005.

1535-3702/06/2316-0741$15.00

significant compensatory downregulation of ET_A receptor density by 50%, correlating with reduced constrictor activity of ET-1 in peripheral vessels (7).

Genetic disruption of the ET_B receptor in mice also significantly increases blood pressure, and circulating ET-1 levels are doubled in heterozygotes compared with wild-type controls (8). Homozygote $ET_B^{-/-}$ knockout mice are viable at birth and can survive for up to 8 weeks, although they display aganglionic megacolon as a result of absence of ganglion neurons together with a pigmentary disorder in their coats (8–11). We have previously shown there is a marked 45% downregulation of ET_A receptors in response to ET_B gene deletion in brains from these $ET_B^{-/-}$ knockout mice (12). Our aim was to use quantitative autoradiography to establish the distribution of ET subtypes in peripheral tissues from wild-type mice and to measure the density of the ET_A subtype in $ET_B^{-/-}$ knockout mice, to test whether deletion of ET_B receptors, leading to reduced plasma clearance, would also reduce ET_A expression in the periphery.

Materials and Methods

Quantitative Autoradiography ET_B Knockout Mouse Model. After euthanasia (carried out in compliance with the NIH Guide for the Care and Use of Laboratory Animals and local and federal animal welfare laws) (10), representative longitudinal cryostat sections (30 μm) were cut from the midline at a level to include the heart, lungs, liver, and kidney from the torsos of four male $WT^{+/+}$ (control) mice, aged 29 ± 3 days and four male $ET_B^{-/-}$ receptor knockout mice, age 25 ± 2 days. The autoradiographic distribution of all ET receptors was determined as previously described (13) by incubating sections for 2 hrs at 23°C with [^{125}I]-ET-1 (0.1 n*M*). ET_A receptors were visualized by incubating adjacent sections with [^{125}I]-ET-1 (0.1 n*M*) in the presence of either 0.1 μ*M* BQ3020 (a concentration calculated to block binding of the radiolabel to the ET_B subtype) or 0.1 μ*M* BQ123 to detect ET_B. Nonspecific binding (NSB) was defined by incubating an additional adjacent section with the radioligand in the presence of unlabeled ET-1 (1 μ*M*). After incubation and washing in ice-cold Tris-HCl buffer to break the equilibrium, the dried sections were apposed to radiation sensitive film, together with calibrated ^{125}I standards from 5 to 7 days, before developing the films. The resulting autoradiograms were analyzed using computer-assisted densitometry (Quantimet 970, Leica, Milton Keynes, UK) as previously described (13). Briefly, each autoradiographic image was digitized. A cursor was used to delineate regions of interest and the integrated optical density measured. When all measurements had been made for a particular section, the threshold for detecting the autoradiogram was increased to produce a template that was used to align the autoradiographic image of an adjacent section used to define the NSB. The second image was digitally subtracted from the first to measure the amount of specific binding. The resulting optical densities were converted to the amount of specifically bound radioligand in amol/mm^2 by interpolation from the standards curve.

Histology and Immunocytochemistry. After exposure to film, the radiolabeled sections were stained with hematoxylin and eosin to facilitate histologic identification of structures in the autoradiograms measured by image analysis. To confirm complete deletion of the $ET_B^{-/-}$ receptor in the knockout mice, immunocytochemistry was carried out by incubating adjacent cryostat sections (30 μm) as previously described (14) using site-directed rabbit antisera raised to the receptor protein sequence, $ET_{B(302–313)}$. Primary antisera were visualized by the peroxidase-antiperoxidase technique.

Results

Distribution of ET_A and ET_B Receptors in $WT^{+/+}$ Mice. The distribution of ET_A and ET_B subtypes in representative longitudinal sections cut at the level of the heart from torso of a $WT^{+/+}$ mouse is shown in Figure 1 and with measured receptor densities in Table 1. The highest densities of ET_A receptors localized to major organs, including the lung (parenchyma), heart (ventricle), and liver (parenchyma). Where resolution was sufficient in the autoradiograms (Fig. 2A and 2C, Table 1), measurements were also made in more discrete regions that comprise mainly one cell type, revealing high densities of ET_A receptors in the smooth muscle layer of the vasculature, such as intrarenal vessels and the smooth muscle layer and epithelial cells of the gastrointestinal tract. In these tissues, the ET_A subtype was more abundant, representing between 60% and 100% of the ET receptors.

ET_B receptors predominated in the medulla of kidney (Fig. 2D, Table 1), with high densities also localizing to glomeruli within the cortex and to the endothelial cell-like sinusoids from the liver (Fig. 2B). Lower densities of ET_B receptors were also present in the lung (parenchyma), heart (ventricle), liver (parenchyma), and the smooth muscle layer of the gastrointestinal tract but not to the epithelial layer (Table 1). In the smooth muscle layer of vessels from the major organs visualized in the autoradiograms, ET_B binding was difficult to detect. Binding to endothelial cells in the vasculature is below the level for detection by film autoradiography and could not be measured.

Quantification of ET_A Receptors in Peripheral Tissues from $ET_B^{-/-}$ Knockout Mice. Specific binding of the ET_B ligand could not be measured above the level of the NSB in all of the knockout animals (Fig. 1). No staining was detected using site-directed antisera to the ET_B receptor, confirming the successful disruption of the protein as expected. ET_A receptor distribution (Fig. 1) in the $ET_B^{-/-}$ knockout mice was similar to the controls, but the density of ET_A receptors was significantly reduced in lung by 39%, although no differences were found in the heart or liver (Fig. 3).

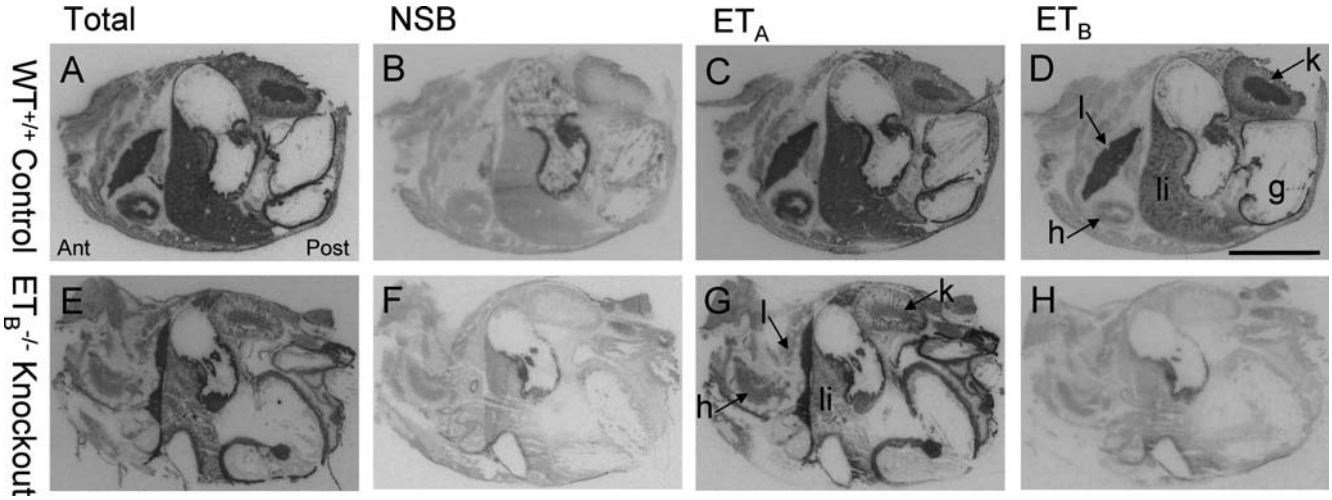

Figure 1. Representative autoradiograms showing localization of ET receptors in consecutive longitudinal cryostat sections cut through the midline of the torso of male $WT^{+/+}$ control (upper panel) or homozygous $ET_B^{-/-}$ knockout mice (lower panel). To visualize all ET receptors (A, E; total), sections were incubated with 0.1 n*M* [^{125}I]-ET-1 alone. Adjacent sections were incubated with the label plus 1 μ*M* ET-1 to define the NSB (B, F). In C and G, a concentration of ET_B ligand, BQ3020 (200 n*M*) was calculated to selectively block [^{125}I]-ET-1 binding to ET_B receptors to reveal the ET_A distribution. In D and H, the concentration of an ET_A selective ligand, BQ123 (200 n*M*), was calculated to block [^{125}I]-ET-1 binding to this subtype to visualize the ET_B distribution. In the control mouse (D), high densities of ET_B binding were detected in kidney and lungs, with lower levels in the liver. In the ET_B knockout, binding could not be detected, as expected, above the NSB, confirming the targeted disruption of the ET_B gene in all tissues examined. ant, anterior; post, posterior; g, gut; h, heart; k, kidney; l, lung; li, liver. Scale bar = 10 mm.

Discussion

Although mice are now widely used to further understand the role of this peptide through target disruption or cell-specific overexpression of key components in the ET system (11), the distribution of ET receptor subtypes has not been extensively studied in this species using whole-body autoradiography. In peripheral tissues, the highest density of ET receptors was present in the lungs as in humans (15) and contained a high proportion of the ET_B subtype, mainly present on endothelial cells (16), consistent with a function in clearing ET-1 from the circulation (4). The sinusoids forming the capillary bed of the liver also express ET_B receptors, which are lined with endothelial cells, consistent with a role in removing ET-1 from the circulation, whereas the parenchyma is mainly ET_A. The kidney also efficiently clears ET-1 from the circulation, and a high density of ET_B binding localized to the glomeruli of the renal cortex and to the medulla. The distribution of the two subtypes in mouse kidney is similar to human renal tissues (17, 18), with comparable ratios of ET_A:ET_B receptors for example in the medulla. The major difference is the high density of ET_B receptors in glomeruli from mice, that are also present in rats, but absent in humans (17).

The ratio of ET_A:ET_B receptors in the ventricle of the mouse heart from the strain used in this study (129/Sv-Ednrb) (10) is comparable to other mice with a different genetic

Table 1. ET_A and ET_B Receptor Density in $WT^{+/+}$ Control Mouse Tissues[a]

Tissue	ET_A (amol/mm^2)	ET_B (amol/mm^2)	Ratio ET_A:ET_B
Lung			
Parenchyma	100.7 ± 5.7	75.3 ± 10.4	57:43
Heart			
Ventricle	75.8 ± 8.3	21.2 ± 6.5	78:22
Liver			
Parenchyma	57.5 ± 11.1	13.6 ± 3.1	81:19
Sinusoid cells	—	33.5 ± 6.0	0:100
Kidney			
Cortex	17.3 ± 2.3	16.8 ± 2.0	51:49
Glomeruli	—	52.0 ± 7.2	0:100
Medulla	31.2 ± 5.8	79.2 ± 5.5	28:72
Intrarenal vessel	40.2 ± 4.9	—	100:0
Gut			
Smooth muscle cells	54.9 ± 4.4	18.2 ± 3.1	75:25
Epithelial cells	44.8 ± 9.7	—	100:0

[a] Each value represents the mean ± standard error of the mean for $n = 4$ mice.

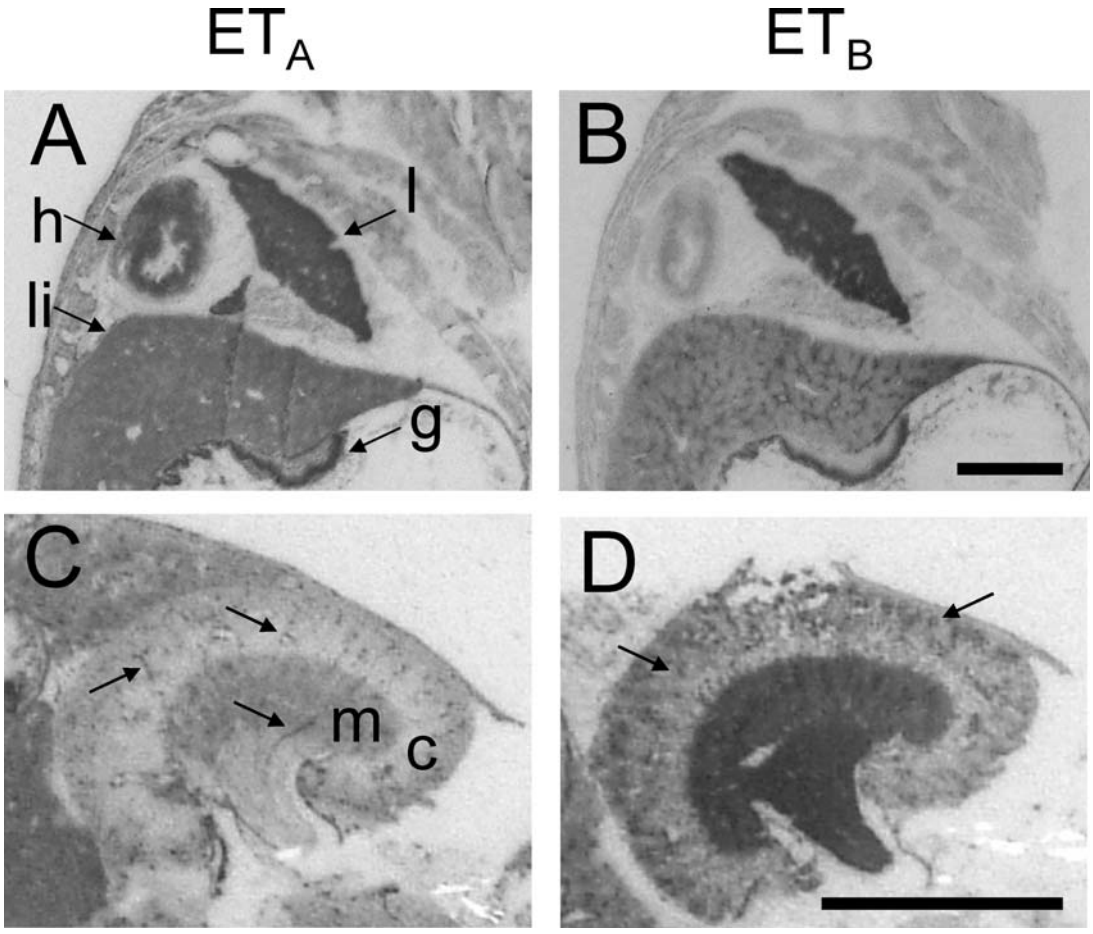

Figure 2. Representative autoradiographic images at higher magnification of ET receptor subtype distribution in the $WT^{+/+}$ control mouse. (A) High densities of ET_A receptors are present in heart, liver, and lungs as well as the smooth muscle and epithelial cell layer of the gastrointestinal tract. ET_A receptors localize to the vasculature such as intrarenal vessels indicated by arrows (C) in both renal cortex and medulla. The ET_B subtype localized to endothelial cell-like sinusoids in liver indicated by arrows (B) with lower densities in lung parenchyma, ventricle of the heart, and to the smooth muscle layer of the gastrointestinal tract but not to the epithelial layer. ET_B receptors predominated in the medulla of kidney (D), with high densities also localizing to glomeruli (arrows) within the cortex. g, gut; h, heart; l, lung; li, liver, c, cortex, m, medulla. Scale bar = 5 mm.

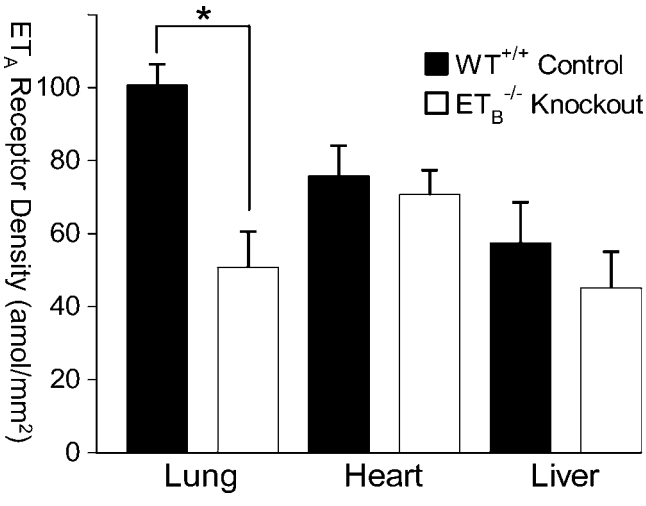

Figure 3. Comparison of ET_A receptor density in peripheral tissues from $ET_B^{-/-}$ knockout mice compared with $WT^{+/+}$ control mice. For each organ, bars represent the mean of 4 mice ± SEM (*$P < 0.003$, Mann-Whitney *U* test).

background, C57/CL6J (19), and to humans (20). ET_A receptors are also the principal isoform in the smooth muscle layer of mouse vasculature such as intrarenal arteries, whereas this is reversed in the airway smooth muscle in which ET_B receptors predominate (10) and form a significant proportion of ET receptors in smooth muscle from the gut. In the tissues examined, the pattern and ratio of ET receptor subtype expression is similar to that seen in man suggesting that disruption of ET receptor subtypes targeted to specific cells using techniques such as the Cre/lox system (16, 21) may have relevance to the development of animal models of human disease.

Interestingly, in tissue where the ET_A receptors predominated (heart and liver), no change was detected in ET_A receptor density in $ET_B^{-/-}$ receptor knockout mice. However, in lung parenchyma where the ratio of ET_A to ET_B receptors is almost equal, suggesting they could be expressed together in the same cell and might be linked by dimerization, there was a significant reduction in ET_A

receptor density. A second possibility to explain downregulation of ET_A receptors in ET_B-rich tissues is that evidence is emerging that ET_B receptor signaling is crucial for embryonic development. Deletion of the ET_B receptor may therefore alter the survival of ET_A-expressing cells, although the evidence in peripheral tissues is that this deletion mainly affects enteric neurons and melanocytes. However, diminished responses to the endogenous agonist after repeated stimulation are an important feature of G-protein signaling, preventing potential damage to the overstimulated cell. A more likely explanation is that the downregulation that has been observed in the lung tissue occurs in response to higher circulating levels of ET-1.

1. Davenport AP, Maguire JJ. Endothelin. Hdbk Exp Pharmacol. 176 (in press).
2. Fukuroda T, Fujikawa T, Ozaki S, Ishikawa K, Yano M, Nishikibe M. Clearance of circulating endothelin-1 by ETB receptors in rats. Biochem Biophys Res Commun 199:1461–1465, 1994.
3. Kuc RE, Karet FE, Davenport AP. Characterization of peptide and nonpeptide antagonists in human kidney. J Cardiovasc Pharmacol 26(Suppl 3):S373–S375, 1995.
4. Johnstrom P, Fryer TD, Richards HK, Harris NG, Barret O, Clark JC, Pickard JD, Davenport AP. Positron emission tomography using ^{18}F-labelled endothelin-1 reveals prevention of binding to cardiac receptors owing to tissue-specific clearance by ET B receptors in vivo. Br J Pharmacol 144:115–22, 2005.
5. Kuc RE, Davenport AP. Endothelin-A-receptors in human aorta and pulmonary arteries are downregulated in patients with cardiovascular disease: an adaptive response to increased levels of endothelin-1? J Cardiovasc Pharmacol 36:S377–S379, 2000.
6. Maguire JJ, Kuc RE, Davenport AP. Affinity and selectivity of PD156707, a novel nonpeptide endothelin antagonist, for human ET(A) and ET(B) receptors. J Pharmacol Exp Ther 280:1102–1108, 1997.
7. Telemaque-Potts, S, Kuc, RE, Yanagisawa, M, Davenport, AP. Tissue-specific modulation of endothelin receptors in a rat model of hypertension. J Cardiovasc Pharmacol 36:S122–S123, 2000.
8. Ohuchi T, Kuwaki T, Ling GY, Dewit D, Ju KH, Onodera M, Cao WH, Yanagisawa M, Kumada M. Elevation of blood pressure by genetic and pharmacological disruption of the ETB receptor in mice. Am J Physiol 276:R1071–R1077, 1999.
9. Hosoda K, Hammer RE, Richardson JA, Baynash AG, Cheung JC, Giaid A, Yanagisawa M. Targeted and natural (piebald-lethal) mutations of endothelin-B receptor gene produce megacolon associated with spotted coat color in mice. Cell 79:1267–1276, 1994.
10. Hay DW, Douglas SA, Ao Z, Moesker RM, Self GJ, Rigby PJ, Luttmann MA, Goldie RG. Differential modulation of endothelin ligand-induced contraction in isolated tracheae from endothelin B (ET(B)) receptor knockout mice. Br J Pharmacol 132:1905–1915, 2001.
11. Kurihara H, Kurihara J, Yazaki, Y. Lessons from gene deletion of endothelin systems. Hdbk Exp Pharmacol 152:141–154, 2001.
12. Davenport AP, Kuc RE. Down-regulation of ETA teceptors in ETB teceptor-deficient Mice. J Cardiovasc Pharmacol 44(Suppl 1):S276–S278, 2004.
13. Davenport AP, Kuc RE. Radioligand-binding and molecular-imaging techniques for the quantitative analysis of established and emerging orphan receptor systems. Methods Mol Biol 306:93–120, 2005.
14. Davenport AP, Kuc RE. Immunocytochemical localization of receptors using light and confocal microscopy with application to the phenotypic characterization of knock-out mice. Methods Mol Biol. 306:155–172, 2005.
15. Davenport AP, Russell FD. Endothelin converting enzymes and endothelin receptor localization in human tissues. Hdbk Exp Pharmacol 152:209–237, 2001.
16. Kelland NF, Bagnall AJ, Gulliver-Sloan FH, Kuc RE, Maguire JJ, Davenport AP, Gray GA, Kotelevtsev YV, Webb DJ. Clearance of circulating endothelin-1 is mediated by the endothelial cell endothelin B receptor. Available at: http://www.pa2online.org/Vol2Issue4abst022P.html. Accessed February 15, 2006.
17. Davenport AP, Kuc RE, Hoskins SL, Karet FE, Fitzgerald F. [125I]-PD151242: a selective ligand for endothelin ETA receptors in human kidney which localizes to renal vasculature. Br J Pharmacol 113:1303–1310, 1994.
18. Karet, FE, Charnock-Jones DS, Harrison-Woolrych ML, O'Reilly G, Davenport AP, Smith SK. Quantification of mRNA in human tissue using fluorescent nested reverse-transcriptase polymerase chain reaction. Anal Biochem 220:384–390, 1994.
19. Wiley KE, Davenport AP. Endothelin receptor pharmacology and function in the mouse: comparison with rat and man. J Cardiovasc Pharmacol 44(Suppl 1):S4–S6, 2004.
20. Molenaar P, O'Reilly G, Sharkey A, Kuc RE, Harding DP, Plumpton C, Gresham GA, Davenport AP. Characterization and localization of endothelin receptor subtypes in the human atrioventricular conducting system and myocardium. Circ Res 72:526–538, 1993.
21. Sauer B. Inducible gene targeting in mice using the Cre/lox system. Methods 14:381–392, 1998.